

Numerical tests of the gauge/gravity duality conjecture for D0-branes at finite temperature and finite N

Masanori HANADA^{abc1}, Yoshifumi HYAKUTAKE^{d2}, Goro ISHIKI^{e3} and Jun NISHIMURA^{fg4}

^a*Stanford Institute for Theoretical Physics, Stanford University, Stanford, CA 94305, USA*

^b*Yukawa Institute for Theoretical Physics, Kyoto University,
Kitashirakawa Oiwakecho, Sakyo-ku, Kyoto 606-8502, Japan*

^c*The Hakubi Center for Advanced Research, Kyoto University,
Yoshida Ushinomiyacho, Sakyo-ku, Kyoto 606-8501, Japan*

^d*College of Science, Ibaraki University, Bunkyo 2-1-1, Mito, Ibaraki 310-8512, Japan*

^e*Center for Integrated Research in Fundamental Science and Engineering (CiRfSE),
Faculty of Pure and Applied Sciences, University of Tsukuba,
Tsukuba, Ibaraki 305-8571, Japan*

^f*KEK Theory Center, High Energy Accelerator Research Organization,
1-1 Oho, Tsukuba, Ibaraki 305-0801, Japan*

^g*Graduate University for Advanced Studies (SOKENDAI),
1-1 Oho, Tsukuba, Ibaraki 305-0801, Japan*

abstract

According to the gauge/gravity duality conjecture, the thermodynamics of gauge theory describing D-branes corresponds to that of black branes in superstring theory. We test this conjecture directly in the case of D0-branes by applying Monte Carlo methods to the corresponding gauge theory, which takes the form of the BFSS matrix quantum mechanics. In particular, we take the continuum limit by extrapolating the UV cutoff to infinity. First we perform simulations at large N so that string loop corrections can be neglected on the gravity side. Our results for the internal energy exhibit the temperature dependence consistent with the prediction including the α' corrections. Next we perform simulations at small N but at lower temperature so that the α' corrections can be neglected on the gravity side. Our results are consistent with the prediction including the leading string loop correction, which suggests that the conjecture holds even at finite N .

¹ E-mail address : hanada@yukawa.kyoto-u.ac.jp

² E-mail address : yoshifumi.hyakutake.phys@vc.ibaraki.ac.jp

³ E-mail address : ishiki@het.ph.tsukuba.ac.jp

⁴ E-mail address : jnishi@post.kek.jp

1 Introduction

One of the most important directions in theoretical physics is to clarify the quantum nature of gravity, which is crucial in understanding the beginning of our Universe and the final state of a black hole. Superstring theory is considered the most promising candidate of a quantum gravity theory due to its UV finiteness in striking contrast to the conventional field theoretical approach to quantum gravity, in which one faces with nonrenormalizable UV divergences. So far, superstring theory is defined only perturbatively around simple backgrounds such as flat spacetime, and it does not seem to be straightforwardly applicable to the studies of a strongly gravitating spacetime such as the black hole geometry. However, this difficulty has been partly surmounted by the discovery of D-branes [1]. Some extremal black holes were constructed by combining different kinds of D-branes, and the origin of their entropy was understood by counting the microstates of the D-branes [2]. Also there are several proposals for nonperturbative formulations of superstring theory based on super Yang-Mills theory in low dimensions [3, 4, 5, 6].

In fact, it is conjectured that superstring theory on the anti-de Sitter background is dual to four-dimensional $\mathcal{N} = 4$ $U(N)$ super Yang-Mills theory [7], which is realized on a stack of N D3-branes. This duality has been generalized in various ways, and it is commonly referred to as the gauge/gravity duality conjecture. The conjecture appears natural considering that D-branes have two descriptions, one from a gravitational viewpoint, and the other from a field theoretical viewpoint. If this conjecture is true even in the presence of quantum effects on the gravity side, the quantum nature of gravity can be studied on a firm ground by investigating the dual gauge theory.

Among various gauge/gravity duality conjectures that have been proposed so far, we are interested in the one that has been studied most intensively, which claims that type II superstring theory in the near horizon limit of the black p -brane geometry is equivalent to a maximally supersymmetric Yang-Mills theory in $(p + 1)$ -dimensions [7, 8]. The super Yang-Mills theory is realized on N D p -branes and it is characterized by the rank of the gauge group N and the 't Hooft coupling $\lambda = g_{\text{YM}}^2 N$. On the gravity side, N is the number of black p -branes, and the 't Hooft coupling is written as $\lambda = (2\pi)^{p-2} \ell_s^{p-3} g_s N$ in terms of the string coupling constant g_s and the string length $\ell_s = \alpha'^{1/2}$. The near horizon limit is taken by $\alpha' \rightarrow 0$ with λ and the energy scale U of the super Yang-Mills theory kept finite. The above gauge/gravity duality has been tested in detail at $N \rightarrow \infty$ and $\lambda \rightarrow \infty$. In this limit, superstring theory is well approximated by supergravity, which makes classical analyses applicable. While the super Yang-Mills theory becomes strongly coupled in this region, one can nevertheless extract the information of BPS states, which are protected by supersymmetry, and confirm the gauge/gravity duality in various ways.

A natural question to ask then is whether the gauge/gravity duality conjecture is valid even for finite λ or finite N , or in a non-supersymmetric setup such as finite temperature. The analyses in these cases are quite difficult, however, because the supergravity approximation is no longer valid on the gravity side and we have to include α' or g_s corrections. Furthermore, the lack of supersymmetry gives rise to all kinds of nonperturbative

corrections to physical quantities on the gauge theory side, which are too hard to handle analytically.

The main purpose of this paper is to test the gauge/gravity duality conjecture for finite N and λ at finite temperature. While it is not possible to calculate finite α' or g_s corrections in superstring theory in general, the corrections to some physical quantities can be extracted by taking account of higher derivative corrections to supergravity perturbatively. For instance, in the case of D0-branes, the internal energy including the leading g_s corrections has recently been evaluated analytically [9, 10]. On the other hand, nonperturbative studies of the super Yang-Mills theory are possible by performing Monte Carlo simulation. In the case of D0-branes, the super Yang-Mills theory takes the form of matrix quantum mechanics for M theory [3, 11], which can be studied with reasonable amount of computational effort. In fact, several groups have studied this model [12, 13, 14, 15, 16, 17, 18, 19, 20, 21, 22, 23, 24, 25] and compared the obtained results with the dual gravity predictions. In particular, finite λ corrections were investigated by Monte Carlo simulation in refs. [16, 18] and more recently in refs. [24, 25], which raised some controversies. In this paper, we first address this issue based on new calculation, which improves our previous analysis [16, 18] by taking the continuum limit.

Then we investigate the $1/N$ corrections by simulating the same system at small N . This turns out to be much more difficult than the studies at large N because of the instability associated with the flat directions in the potential. The bound state of D0-branes is stable at large N , but it becomes only meta-stable at sufficiently low temperature for small N . We extract the internal energy of the meta-stable bound states by introducing a cutoff on the extent of the D0-brane distribution, which is chosen in such a way that the obtained result does not depend on it within a certain region. Our results obtained in this way turn out to be consistent with the analytic result obtained on the gravity side including the leading g_s corrections. This suggests that the gauge/gravity duality holds even at finite N . In fact, the instability at finite N can be understood also on the gravity side. Some of the results are reported briefly in our previous publication [21].

The rest of this paper is organized as follows. In section 2 we give an overview of the black 0-brane thermodynamics, and discuss how finite λ and finite N corrections appear in the internal energy of the D0-branes. In section 3 we explain how we study the D0-brane quantum mechanics by Monte Carlo simulation. In section 4 we provide numerical tests of the gauge/gravity duality including finite λ and finite N corrections. Section 5 is devoted to a summary and discussions.

2 Brief review on the black 0-brane thermodynamics

In this section we briefly review the thermodynamics of the black 0-brane in type IIA superstring theory, which appears in the gauge/gravity duality we are going to test. In particular, we derive an expression for the quantity that should be compared with the internal energy of the dual gauge theory calculable by Monte Carlo methods. Corresponding

to finite λ and finite N corrections on the gauge theory side, we need to consider how the black 0-brane thermodynamics is affected by the higher derivative corrections to the low-energy effective action of type IIA superstring theory.

2.1 The effects of higher derivative corrections on the black 0-brane thermodynamics

In the low energy limit, the scattering amplitudes of strings in type II superstring theory can be reproduced correctly by the type II supergravity action. However, if we go beyond the low energy limit, we have to take into account the effects due to the finite length ℓ_s of strings (α' corrections) and the effects of string loops (g_s corrections). In general, these effects can be extracted by considering the scattering amplitudes of strings associated with a Riemann surface with genus n and expanding them with respect to external momenta [26, 27]. The number of external momenta in the expansion raises the power of α' , whereas the genus n gives the power of g_s^2 . The corrections to the type II supergravity action due to these effects are represented by higher derivative terms, and they are organized in the form of a double expansion with respect to α' and g_s . Below, we discuss some qualitative features of the higher derivative terms in type IIA superstring theory.

Treating the type IIA superstring theory perturbatively with respect to two parameters $\alpha' = \ell_s^2$ and the dilaton coupling $g_s e^\phi$, one can write its effective action formally as

$$S = \frac{1}{2\kappa_{10}^2} \int d^{10}x \sqrt{-g} e^{-2\phi} \left(\mathcal{O}^{(0)} + \sum_{m,n} \ell_s^{2m} (g_s e^\phi)^{2n} \mathcal{O}^{(m,n)} \right), \quad (2.1)$$

with an overall coefficient given by $2\kappa_{10}^2 = (2\pi)^7 \ell_s^8 g_s^2$. Here $\mathcal{O}^{(0)}$ represents the terms with mass dimension 2 that appear in the type IIA supergravity action, and $\mathcal{O}^{(m,n)}$ represents higher derivative corrections with mass dimension $(2m+2)$. All these terms are written in terms of the massless fields in the type IIA superstring theory such as the graviton $g_{\mu\nu}$, the dilaton ϕ and the R-R 1-form potential C_μ . The structure of the higher derivative terms can be determined by explicit calculations of scattering amplitudes, which show that the ℓ_s^6 and $\ell_s^6 g_s^2$ terms appear as the leading corrections, respectively, at the tree level and at the one-loop level. It is also known that these terms do not appear from higher loops. Thus we only have terms in eq. (2.1) with $m \geq 3$ for $n = 0, 1$ and with $m > 3$ for $n \geq 2$ [28].

The equations of motion that one obtains from the effective action (2.1) can also be expanded in a power series as

$$\mathcal{E} = \mathcal{E}^{(0)} + \sum_{m,n} \ell_s^{2m} (g_s e^\phi)^{2n} \mathcal{E}^{(m,n)} = 0, \quad (2.2)$$

omitting the tensor indices for simplicity. Here $\mathcal{E}^{(0)}$ represents the part obtained from the type IIA supergravity, and $\mathcal{E}^{(m,n)}$ represents the part obtained from the high derivative corrections. In order to solve the above equations of motion for the black 0-brane, we make

a general ansatz for $g_{\mu\nu}$, ϕ and C_μ respecting SO(9) rotational symmetry as [9]

$$\begin{aligned}
ds^2 &= -H_1^{-1} H_2^{\frac{1}{2}} F_1 dt^2 + H_2^{\frac{1}{2}} F_1^{-1} dr^2 + H_2^{\frac{1}{2}} r^2 d\Omega_8^2, \\
e^\phi &= H_2^{\frac{3}{4}}, \quad C = \sqrt{1 + \alpha^7} (H_2 H_3)^{-\frac{1}{2}} dt, \\
H_i(r) &= 1 + \frac{r_-^7}{r^7} + \sum_{m,n} \ell_s^{2m} g_s^{2n} H_i^{(m,n)}(r), \\
F_1(r) &= 1 - \frac{(r-\alpha)^7}{r^7} + \sum_{m,n} \ell_s^{2m} g_s^{2n} F_1^{(m,n)}(r),
\end{aligned} \tag{2.3}$$

which involves four unknown functions $H_i(r)$ ($i = 1, 2, 3$) and $F_1(r)$. The leading behaviors of H_i and F_1 are fixed by using the solution of $\mathcal{E}^{(0)} = 0$ which are asymptotically flat, and they involve two parameters r_- and α . As we will see below, r_- and α are related to the mass and the charge of the black 0-brane. The subleading terms described by the functions $H_i^{(m,n)}$ and $F_1^{(m,n)}$ can be obtained by solving eq. (2.2) order by order. Note that the functions for $(m, n) = (3, 0)$ and $(m, n) = (3, 1)$ can be obtained independently of the other unknowns since they are the leading corrections, respectively, at the tree level and at the one-loop level.

The event horizon r_H , which is defined by $F_1(r_H) = 0$, can be obtained perturbatively as $r_H = r_- \alpha + \dots$. Then the Hawking temperature \tilde{T} can be obtained by requiring the absence of conical singularity in the Euclidean geometry at the event horizon as⁵

$$\tilde{T} = \frac{1}{4\pi} H_1^{-\frac{1}{2}} \frac{dF_1}{dr} \Big|_{r_H} = \frac{7(r_- \alpha)^{\frac{5}{2}}}{4\pi r_-^{\frac{7}{2}} \sqrt{1 + \alpha^7}} \left(1 + \sum_{m,n} \ell_s^{2m} g_s^{2n} \tilde{T}^{(m,n)} \right), \tag{2.4}$$

where $\tilde{T}^{(m,n)}$ can be determined once the solution is obtained. Since the metric (2.3) is asymptotically flat, the mass \tilde{M} of the black 0-brane can be evaluated by using the ADM mass formula and the charge \tilde{Q} can be calculated by integrating the R-R flux⁶. They can be written formally as

$$\tilde{M} = \frac{V_{S^8}}{2\kappa_{10}^2} (r_- \alpha)^7 \left(\frac{7 + 8\alpha^7}{\alpha^7} + \sum_{m,n} \ell_s^{2m} g_s^{2n} \tilde{M}^{(m,n)} \right), \tag{2.5}$$

$$\tilde{Q} = \frac{V_{S^8}}{2\kappa_{10}^2} (r_- \alpha)^7 \left(\frac{7\sqrt{1 + \alpha^7}}{\alpha^7} + \sum_{m,n} \ell_s^{2m} g_s^{2n} \tilde{Q}^{(m,n)} \right), \tag{2.6}$$

where $V_{S^8} = \frac{2\pi^{9/2}}{\Gamma(9/2)} = \frac{2(2\pi)^4}{7 \cdot 15}$ is the volume of S^8 . The internal energy of N D0-branes $\tilde{E} = \tilde{M} - \tilde{Q}$, which is identified as the difference between the mass and the charge, can be

⁵Here we reserve the variables such as T , E and U_0 without tildes for dimensionless quantities to be defined in (2.14).

⁶The integrands for the ADM mass and the R-R charge have corrections due to the higher derivative terms, which vanish at $r = \infty$ [10].

obtained from (2.5) and (2.6) as

$$\tilde{E} = \frac{V_{S^8}}{2\kappa_{10}^2} (r_- \alpha)^7 \left(\frac{1 + 8\sqrt{1 + \alpha^7}}{1 + \sqrt{1 + \alpha^7}} + \sum_{m,n} \ell_s^{2m} g_s^{2n} \tilde{E}^{(m,n)} \right), \quad (2.7)$$

where $\tilde{E}^{(m,n)}$ has mass dimension $2m$.

2.2 Black 0-brane thermodynamics at large N

Let us first consider the supergravity approximation, which is valid when the curvature radius is large compared to ℓ_s and the effective coupling $g_s e^\phi$ is small. Neglecting higher derivative corrections in eqs. (2.4) and (2.7), the temperature and the internal energy of the black 0-brane are obtained as

$$\tilde{T} = \frac{7(r_- \alpha)^{\frac{5}{2}}}{4\pi r_-^{\frac{7}{2}} \sqrt{1 + \alpha^7}}, \quad \tilde{E} = \frac{V_{S^8}}{2\kappa_{10}^2} (r_- \alpha)^7 \frac{1 + 8\sqrt{1 + \alpha^7}}{1 + \sqrt{1 + \alpha^7}}, \quad (2.8)$$

where r_- and α are the parameters of the classical black 0-brane. The extremal limit corresponds to $\alpha \rightarrow 0$ and $r_-^7 \rightarrow (2\pi)^2 15\pi g_s N \ell_s^7$, where the latter follows from the former using $\tilde{Q} = N/(\ell_s g_s)$ and (2.6). In that limit, the event horizon $r_H = r_- \alpha$, the temperature \tilde{T} and the internal energy \tilde{E} all vanish as long as r_- is kept finite.

The gauge/gravity duality holds in the near horizon limit [7, 8], which is given in the present case by

$$\ell_s \rightarrow 0 \quad \text{with} \quad \tilde{U}_0 \equiv \frac{r_H}{\ell_s^2} \quad \text{and} \quad \lambda = \frac{g_s N}{(2\pi)^2 \ell_s^3} \quad \text{fixed.} \quad (2.9)$$

Note that the gravitational coupling κ_{10}^2 goes to zero when $\ell_s \rightarrow 0$ with the 't Hooft coupling $\lambda = g_{\text{YM}}^2 N$ fixed. This means that the gauge theory on the D0-branes decouples from the bulk gravity. On the other hand, the parameter \tilde{U}_0 in (2.9) is proportional to the product of the string tension $1/2\pi\ell_s^2$ and the typical length r_H , which represents the gauge boson mass in the gauge theory. Therefore, fixing \tilde{U}_0 in the limit corresponds to keeping the energy scale of the dual gauge theory finite. Let us also mention that the limit (2.9) can be rewritten in terms of α and r_- , as

$$\alpha \rightarrow 0, \quad \frac{r_-^2}{\alpha^5} \rightarrow (2\pi)^4 15\pi \lambda \tilde{U}_0^{-5}, \quad \frac{2\kappa_{10}^2}{(r_- \alpha)^7} \rightarrow \frac{(2\pi)^{11} \lambda^2 \tilde{U}_0^{-7}}{N^2}. \quad (2.10)$$

Since $\alpha \rightarrow 0$ and $r_- \rightarrow 0$, the near horizon limit may be regarded as a special case of the near extremal limit, in which the temperature \tilde{T} and the internal energy \tilde{E} are kept finite.

In the near horizon limit, physical quantities can be expressed in terms of \tilde{U}_0 and λ . Introducing a rescaled coordinate $U = r/\ell_s^2$, we can rewrite the solution (2.3) as [8]

$$ds^2 = \ell_s^2 \left(-H^{-\frac{1}{2}} F dt^2 + H^{\frac{1}{2}} F^{-1} dU^2 + H^{\frac{1}{2}} U^2 d\Omega_8^2 \right),$$

$$\begin{aligned}
e^\phi &= \ell_s^{-3} H^{\frac{3}{4}}, \quad C = \ell_s^4 H^{-1} dt, \\
H &= \frac{(2\pi)^4 15\pi\lambda}{U^7}, \quad F = 1 - \frac{\tilde{U}_0^7}{U^7}.
\end{aligned} \tag{2.11}$$

Taking the near horizon limit in eq. (2.8), we obtain

$$T = a_1 U_0^{\frac{5}{2}}, \quad a_1 = \frac{7}{16\pi^3 \sqrt{15\pi}}, \tag{2.12}$$

$$\frac{E}{N^2} = \frac{18}{7^3} a_1^2 U_0^7 = \frac{18}{7^3} a_1^{-\frac{4}{5}} T^{\frac{14}{5}} \sim 7.41 T^{2.8}, \tag{2.13}$$

where we have defined the dimensionless quantities

$$T = \frac{\tilde{T}}{\lambda^{\frac{1}{3}}}, \quad U_0 = \frac{\tilde{U}_0}{\lambda^{\frac{1}{3}}}, \quad E = \frac{\tilde{E}}{\lambda^{\frac{1}{3}}}. \tag{2.14}$$

Since the curvature radius ρ and the effective coupling $g_s e^\phi$ around the event horizon are estimated as

$$\frac{\ell_s}{\rho} \sim U_0^{\frac{3}{4}}, \quad g_s e^\phi \sim \frac{1}{N} U_0^{-\frac{21}{4}}, \tag{2.15}$$

the result (2.13) for the internal energy is valid when $U_0 \ll 1$ and $U_0^{-\frac{21}{4}} \ll N$, which translates to $T \ll 1$ and $T^{-\frac{21}{10}} \ll N$ due to (2.12).

When N is large but $T \sim O(1)$, ℓ_s/ρ is no longer small, and all the higher order terms with $n = 0$ remain in (2.4) and (2.7). Therefore, eq. (2.13) should be replaced by

$$\frac{E}{N^2} = 7.41 T^{2.8} \left(1 + \sum_{m \geq 3} c_{m,0} T^{\frac{3m}{5}} \right) = 7.41 T^{2.8} + a T^{4.6} + \tilde{a} T^{5.8} + \dots, \tag{2.16}$$

where the second term comes from the leading α' correction with $(m, n) = (3, 0)$ and the third term comes from the next-leading α' correction with $(m, n) = (5, 0)$. The absence of $c_{4,0}$ follows from some knowledge [28] on the structure of the effective action (2.1). The explicit values of the non-zero coefficients $c_{m,0}$ are not known so far, however.

In fact, the internal energy of the black 0-brane is affected by the Hawking radiation, which has not been taken into account in (2.7). However, the energy loss through the Hawking radiation can be neglected in the near horizon limit, as we show in appendix A. This is reasonable since the near horizon limit implies the near extremal limit as well.

2.3 Black 0-brane thermodynamics at finite N

Let us move on to the case with finite N . Since the effective coupling $g_s e^\phi$ given by (2.15) can no longer be neglected, all the higher order terms in eqs. (2.4) and (2.7) remain. Using (2.15), each dimensionless term in (2.4) and (2.7) behaves as

$$\ell_s^{2m} g_s^{2n} \tilde{E}^{(m,n)} \sim \frac{1}{N^{2n}} U_0^{\frac{3m-21n}{2}}, \quad \ell_s^{2m} g_s^{2n} \tilde{T}^{(m,n)} \sim \frac{1}{N^{2n}} U_0^{\frac{3m-21n}{2}}. \tag{2.17}$$

Therefore, the internal energy of the black 0-brane in the near horizon limit is obtained as

$$\frac{E}{N^2} = 7.41 T^{2.8} \left(1 + \sum_{m,n} \frac{c_{m,n}}{N^{2n}} T^{\frac{3m-21n}{5}} \right). \quad (2.18)$$

The coefficients $c_{m,n}$ can be determined, in principle, by solving the equations of motion (2.2) that can be derived from the explicit form of the effective action (2.1). Using some knowledge [28] on the structure of the effective action (2.1), we have $c_{m,1} \neq 0$ only for $m = 3, 6, \dots$ and $c_{m,2} \neq 0$ only for $m = 5, 6, \dots$, etc..

In general, it is difficult to obtain the higher derivative corrections in the effective action (2.1). There exists one exception, however, which is the leading correction at one loop corresponding to $(m, n) = (3, 1)$. In this case, the correction can be obtained [10] by uplifting the black 0-brane solution to the M-wave solution in eleven dimensions, which is purely geometrical. Since higher curvature corrections in eleven dimensions are well-known [29, 30, 31, 32, 33], it is possible to derive the equations of motion and solve them. Using this result, the internal energy including the leading $1/N^2$ correction can be obtained explicitly as [10]

$$\frac{E}{N^2} = 7.41 T^{\frac{14}{5}} - \frac{5.77}{N^2} T^{\frac{2}{5}}. \quad (2.19)$$

(See appendix B for a review on the derivation.)

Thus we find that the internal energy can be expanded with respect to T and $1/N$ as

$$\frac{E}{N^2} = (7.41 T^{2.8} + a T^{4.6} + \tilde{a} T^{5.8} + \dots) + (-5.77 T^{0.4} + b T^{2.2} + \dots) \frac{1}{N^2} + O\left(\frac{1}{N^4}\right), \quad (2.20)$$

where $a T^{4.6}$ and $\tilde{a} T^{5.8}$ correspond to the ℓ_s^6 terms and the ℓ_s^{10} terms, respectively, at the tree level, while $b T^{2.2}$ comes from the $\ell_s^{12} g_s^2$ terms at the one-loop level.

3 D0-brane quantum mechanics

According to the gauge/gravity duality conjecture, the thermodynamics of the black 0-brane corresponds to that of the gauge theory describing the D0-brane, which takes the form of the BFSS matrix quantum mechanics. In order to investigate the thermodynamics, we use the Euclidean time and compactify it with the periodicity $\beta = 1/\tilde{T}$. Then the action of D0-brane quantum mechanics at finite temperature \tilde{T} is given by

$$S = \frac{1}{g_{\text{YM}}^2} \int_0^\beta dt \text{Tr} \left\{ \frac{1}{2} (D_t X_i)^2 - \frac{1}{4} [X_i, X_j]^2 + \frac{1}{2} \psi_\alpha D_t \psi_\alpha - \frac{1}{2} \psi_\alpha \gamma_i^{\alpha\beta} [X_i, \psi_\beta] \right\}, \quad (3.1)$$

which can be obtained formally by dimensionally reducing the action of $(9+1)\text{d } \mathcal{N} = 1$ $U(N)$ super Yang-Mills theory to $(0+1)$ dimension. We have introduced $X_i(t)$ ($i = 1, \dots, 9$)

and $\psi_\alpha(t)$ ($\alpha = 1, \dots, 16$), which are bosonic and fermionic $N \times N$ Hermitian matrices, respectively, and the covariant derivative $D_t = \partial_t - i[A(t), \cdot]$ is defined using the $U(N)$ gauge field $A(t)$. The bosonic variables obey periodic boundary conditions $X_i(t+\beta) = X_i(t)$, $A(t+\beta) = A(t)$, whereas the fermionic variables obey anti-periodic boundary conditions $\psi_\alpha(t+\beta) = -\psi_\alpha(t)$. The 16×16 matrices γ_i in (3.1) act on spinor indices and satisfy the Euclidean Clifford algebra $\{\gamma_i, \gamma_j\} = 2\delta_{ij}$.

The 't Hooft coupling $\lambda = g_{\text{YM}}^2 N$ corresponds to λ defined in (2.9) on the dual gravity side. Since the coupling constant g_{YM}^2 in the action (3.1) has mass dimension 3, all dimensionful quantities can be measured in units of λ as we did in (2.14). Note that the expansion (2.20) is valid when $T \ll 1$ and $T^{-\frac{21}{10}} \ll N$. In particular, the first inequality implies that λ should be large for fixed temperature \tilde{T} . This implies that we need to study the strong coupling dynamics of the D0-brane quantum mechanics in order to test the gauge/gravity duality. For that purpose, we apply Monte Carlo methods analogous to the ones used in lattice QCD.

3.1 Putting the theory on a computer

In order to apply Monte Carlo methods, we have to put the D0-brane quantum mechanics (3.1) on a computer. It is not possible to do it, however, respecting all the maximal supersymmetry generated by 16 supercharges, which the theory has at zero temperature. For instance, if one discretizes the time direction, one cannot maintain all the supersymmetry, since successive supersymmetry transformations induce a translation in time direction, which is broken by the discretization. The lack of exact symmetry in quantum field theories typically necessitates fine tuning in taking the continuum limit due to UV divergences. This does not occur, however, in the present case since the system is just a quantum mechanics, which is UV finite. Here, instead of discretizing the time direction, we expand the functions of t in Fourier modes and introduce a mode cutoff Λ after fixing the gauge symmetry [34]. Since the higher Fourier modes omitted in our calculations are suppressed by the kinetic term, the approach to $\Lambda = \infty$ is expected to be fast.

We fix the gauge symmetry by the static diagonal gauge

$$A(t) = \frac{1}{\beta} \text{diag}(\alpha_1, \dots, \alpha_N), \quad (3.2)$$

where α_a are chosen to satisfy the constraint⁷

$$-\pi < \alpha_a \leq \pi. \quad (3.3)$$

This constraint is needed to fix the symmetry under large gauge transformations⁸. The

⁷In actual simulation, we replace the constraint by $\max_a(\alpha_a) - \min_a(\alpha_a) \leq 2\pi$. This is practically equivalent to (3.3) unless α_a is distributed in the whole region (3.3), which occurs only at very low temperature.

⁸The gauge transformation acts on the gauge field as $A(t) \rightarrow \Omega(t)^{-1} A(t) \Omega(t) + i\Omega(t)^{-1} \partial_t \Omega(t)$, where $\Omega(t)$ is an $N \times N$ unitary matrix which satisfies the periodic boundary condition $\Omega(t+\beta) = \Omega(t)$. After taking the static diagonal gauge, one still has to fix the residual symmetry under large gauge transformations, which correspond to $\Omega(t) = \text{diag}(e^{2\pi i n_1 t/\beta}, \dots, e^{2\pi i n_N t/\beta})$ with n_1, \dots, n_N being integers.

Faddeev-Popov term associated with this gauge fixing condition is given by

$$S_{\text{FP}} = - \sum_{a < b} 2 \ln \left| \sin \frac{\alpha_a - \alpha_b}{2} \right|, \quad (3.4)$$

which we add to the action (3.1). The integration measure for α_a is taken to be uniform.

Once we fix the gauge symmetry, we can introduce the momentum cutoff Λ for the Fourier modes of $X_i(t)$ and $\psi_\alpha(t)$. Since the bosonic matrices $X_i(t)$ obey periodic boundary conditions, they are expanded as

$$X_i^{ab}(t) = \sum_{n=-\Lambda}^{\Lambda} \tilde{X}_{in}^{ab} e^{in\omega t}, \quad (3.5)$$

where $\omega = 2\pi/\beta$, and n runs over integers⁹. On the other hand, the fermionic matrices $\psi_\alpha(t)$, which obey anti-periodic boundary conditions, are expanded as

$$\psi_\alpha^{ab}(t) = \sum_{r=-(\Lambda-1/2)}^{\Lambda-1/2} \tilde{\psi}_{\alpha r}^{ab} e^{ir\omega t}, \quad (3.6)$$

where r runs over half-integers. By using a shorthand notation

$$\left(f^{(1)} \dots f^{(p)} \right)_n \equiv \sum_{k_1 + \dots + k_p = n} f_{k_1}^{(1)} \dots f_{k_p}^{(p)}, \quad (3.7)$$

the action (3.1) can be expressed as $S = S_b + S_f$, where

$$S_b = N\beta \left[\frac{1}{2} \sum_{n=-\Lambda}^{\Lambda} \left(n\omega - \frac{\alpha_a - \alpha_b}{\beta} \right)^2 \tilde{X}_{i,-n}^{ba} \tilde{X}_{in}^{ab} - \frac{1}{4} \text{Tr} \left([\tilde{X}_i, \tilde{X}_j]^2 \right)_0 \right], \quad (3.8)$$

$$S_f = \frac{1}{2} N\beta \left[\sum_{r=-(\Lambda-1/2)}^{\Lambda-1/2} i \left(r\omega - \frac{\alpha_a - \alpha_b}{\beta} \right) \tilde{\psi}_{\alpha,-r}^{ba} \tilde{\psi}_{\alpha r}^{ab} - (\gamma_i)_{\alpha\beta} \text{Tr} \left(\tilde{\psi}_\alpha [\tilde{X}_i, \tilde{\psi}_\beta] \right)_0 \right]. \quad (3.9)$$

This action is written in terms of a finite number of variables α_a , \tilde{X}_{in}^{ab} and $\tilde{\psi}_{\alpha r}^{ab}$, and hence it can be dealt with on a computer. The continuum limit is realized by sending the cutoff Λ to infinity.

The fermionic degrees of freedom are treated in the following way. Note that the fermionic action S_f can be written as $S_f = \frac{1}{2} \mathcal{M}_{A\alpha r, B\beta s} \tilde{\psi}_{\alpha r}^A \tilde{\psi}_{\beta s}^B$, where we have expanded $\tilde{\psi}_{\alpha r}$ in terms of the generators t^A of $U(N)$ as $\tilde{\psi}_{\alpha r} = \sum_{A=1}^{N^2} \tilde{\psi}_{\alpha r}^A t^A$. By integrating out the fermionic variables, the partition function can be written as

$$Z = \int dX d\alpha d\psi e^{-S_b - S_f} = \int dX d\alpha \text{Pf} \mathcal{M} e^{-S_b}, \quad (3.10)$$

⁹Note that a large gauge transformation shifts the momentum of the mode \tilde{X}_{in}^{ab} as $n \rightarrow n - n_a + n_b$. Therefore, one needs to fix the symmetry under large gauge transformations in order for the momentum cutoff to make sense.

where $\text{Pf}\mathcal{M}$ represents the Pfaffian of \mathcal{M} , which is complex in general and is denoted as $\text{Pf}\mathcal{M} = |\text{Pf}\mathcal{M}| e^{i\Gamma}$. Since Monte Carlo simulation is applicable only when the path integral has a positive semi-definite integrand, we omit the phase factor $e^{i\Gamma}$ and define the expectation value of $\mathcal{O}(X, \alpha)$ for the phase-quenched model as

$$\left\langle \mathcal{O}(X, \alpha) \right\rangle_{\text{phase-quenched}} \equiv \frac{\int dX d\alpha \mathcal{O}(X, \alpha) |\text{Pf}\mathcal{M}| e^{-S_b}}{\int dX d\alpha |\text{Pf}\mathcal{M}| e^{-S_b}}. \quad (3.11)$$

Then, the expectation value with respect to the original theory (3.10) is given by

$$\left\langle \mathcal{O}(X, \alpha) \right\rangle = \frac{\left\langle \mathcal{O}(X, \alpha) e^{i\Gamma} \right\rangle_{\text{phase-quenched}}}{\left\langle e^{i\Gamma} \right\rangle_{\text{phase-quenched}}}. \quad (3.12)$$

When $e^{i\Gamma}$ fluctuates rapidly in the simulation of the phase-quenched model, it is difficult to evaluate (3.12) since both the denominator and the numerator become very small, and the number of configurations needed to obtain the ratio with sufficient accuracy becomes huge. This technical problem is called the sign problem.

In the present system, however, it has been reported that the fluctuation of $e^{i\Gamma}$ is strongly suppressed at both high temperature and low temperature, and that it can be neglected throughout the whole temperature region [23, 25]. This can be understood as follows. At high temperature, the high temperature expansion becomes applicable [35], which implies that the dynamics of X and α in the Pfaffian becomes perturbative. Therefore, the fluctuation of $e^{i\Gamma}$ becomes less important at high temperature. At low temperature, on the other hand, the dynamics is dominated by the low momentum modes, for which the kinetic term (the first term) in (3.9) can be neglected. If we omit the kinetic term, we can show that the Pfaffian becomes real. Thus, the effects of $e^{i\Gamma}$ can be neglected also at low temperature, which is supported by some numerical evidence [19]. In the present work, we simply omit the phase factor $e^{i\Gamma}$, and use (3.11) to calculate the VEV of observables. See appendix B of ref. [19] for the details of our algorithm for Monte Carlo simulation.

Let us also comment on how we treat the zero modes. Note that the constant modes $X_i(t) = x_i \mathbf{1}_N$ ($x_i \in \mathbb{R}$) of the trace part does not appear in the action (3.1). These modes should be omitted in the path integral (3.10). We can extract these modes from a general configuration by

$$x_i = \frac{1}{N\beta} \int_0^\beta dt \text{Tr}(X_i(t)). \quad (3.13)$$

In what follows, we assume that these zero modes are fixed by the constraint $x_i = 0$ for $i = 1, \dots, 9$. In Monte Carlo simulation, even if we start from a configuration satisfying the constraint, x_i can become nonzero as the simulation proceeds due to accumulation of round-off errors. We avoid this by making a projection $X_i(t) \mapsto X'_i(t) = X_i(t) - x_i \mathbf{1}_N$.

3.2 Calculation of the internal energy

The internal energy $E = -\frac{\partial}{\partial\beta} \ln Z$ of the D0-brane quantum mechanics can be calculated using the formula

$$E = -3T \left(\langle S_b \rangle - \frac{9}{2} \left\{ (2\Lambda + 1)N^2 - 1 \right\} \right) , \quad (3.14)$$

which can be obtained by adapting the one used in the lattice formulation [36] to the present momentum cutoff formulation. (See appendix C for the derivation.)

A peculiar aspect of the D0-brane quantum mechanics is that the action (3.1) has flat directions $[X_i, X_j] = 0$. These are lifted by quantum corrections in the case of the bosonic model, in which fermionic degrees of freedom are omitted [37]. However, in the supersymmetric model, the flat directions are not lifted by quantum corrections due to supersymmetry. As a result, the supersymmetric model contains scattering states, which form the continuous branch of the energy spectrum, in addition to the normalizable energy eigenstates, which form the discrete branch of the spectrum.¹⁰ Therefore, the path integral (3.10) is ill-defined as it stands, and we need to consider how to make sense out of it.

In the large- N limit, the path integral (3.10) becomes well-defined analogously to the well-known example of the Φ^3 model [40]. In this case, we may naturally consider that the well-defined path integral (3.10) actually represents the thermodynamics of the normalizable states only.

The situation becomes subtle at finite N . Suppose we prepare an initial state with $X_i \sim 0$ having sufficiently low energy and let it evolve in time quantum mechanically. It is expected from the Monte Carlo simulation discussed in section 4.2 that the size $\mathcal{O} = \frac{1}{N} \text{Tr}(X_i)^2$ of the state fluctuates for a while around some finite value depending on the initial state, and eventually starts to diverge. These meta-stable states are linear combinations of normalizable states and scattering states. However, if they are long-lived, we can still think of their thermodynamics by introducing a cutoff $\mathcal{O} \leq R_{\text{cut}}^2$, where R_{cut}^2 should be chosen to be the typical size of the meta-stable states for a given energy. This can be achieved in the path integral formalism by replacing the partition function (3.10) by

$$Z = \int dX d\alpha d\psi e^{-S_b - S_t} \theta(R_{\text{cut}}^2 - R_{\text{max}}^2) = \int dX d\alpha \text{Pf} \mathcal{M} e^{-S_b} \theta(R_{\text{cut}}^2 - R_{\text{max}}^2) , \quad (3.15)$$

where $\theta(x)$ is the Heaviside step function and we have defined

$$R_{\text{max}}^2 \equiv \frac{1}{N} \max_{0 \leq t \leq \beta} \sum_{i=1}^9 \text{Tr}(X_i(t)^2) . \quad (3.16)$$

¹⁰In ref. [38], the discrete branch of the spectrum is shown to have a new energy scale proportional to $N^{-5/9}$ based on the effective Hamiltonian for the relevant $\mathcal{O}(N)$ degrees of freedom in the flat directions. Based on this observation, the particular power “2.8” of the leading behavior in (2.16) has been understood theoretically on the gauge theory side. See also ref. [39] for related work on supersymmetric models with 4 and 8 supercharges.

It is expected that the internal energy of the cutoff system (3.15) becomes independent of R_{cut}^2 within some region, and the internal energy obtained in that region can be interpreted as the average internal energy of the meta-stable states for the T and N corresponding to the partition function (3.15). The typical size of the meta-stable states can be identified with the lower end of the region of R_{cut}^2 within which the internal energy is constant. Note that the partition function (3.15) does not represent the thermodynamics of the normalizable states only unlike the case with $N = \infty$. Therefore, there is no guarantee that the specific heat $C = \frac{dE}{dT}$ corresponding to the internal energy E defined in this way becomes positive.

Since the N eigenvalues of X_i represent the position of the D0-branes, the meta-stable states can be interpreted as the bound states of D0-branes, which form a black hole. Therefore, it is expected that the internal energy defined above corresponds to the internal energy (2.20) of the black hole. Indeed the black hole is stable in the large- N limit, but it becomes meta-stable at finite N due to quantum effects corresponding to $1/N^2$ corrections. This can be seen in (2.19), for instance, where the leading $1/N^2$ correction makes the specific heat negative at sufficiently low T . This instability can be understood physically as caused by the repulsive force acting on a test particle near the event horizon due to the quantum gravity effects at small distances [9].

4 Numerical tests of the gauge/gravity duality

In this section we provide numerical tests of the gauge/gravity duality including finite λ and finite N corrections, which correspond to the α' and string loop corrections, respectively, on the gravity side. These corrections are discussed separately in sections 4.1 and 4.2.

4.1 Test including α' corrections

In this section we provide a test of the gauge/gravity duality in the large- N limit. For that purpose, we perform Monte Carlo simulation of the D0-brane quantum mechanics (3.1) at large N and compare the results with the prediction (2.16) obtained on the gravity side. As long as $N > N_c(T)$, where $N_c(T)$ is some critical value depending on T , the instability mentioned in the previous section does not show up practically during Monte Carlo simulation, and we can calculate various observables by taking an average in a straightforward manner. The critical value is found to behave as $N_c(T) \sim 6/T$ at $T \gtrsim 0.5$ [16], which makes the lower T region difficult to study.

In ref. [18], the results obtained by Monte Carlo simulation with $N \leq 17$ and $\Lambda \leq 8$ were compared with the prediction including α' corrections. The numerical data were fitted by an ansatz $E/N^2 = 7.41 T^{2.8} + a T^p$ with $p = 4.58(3)$ and $a = -5.55(7)$, which is consistent with the prediction $p = 4.6$ from the gravity side. However, a recent paper [24] repeated the analysis including data points at lower T with $N = 32$ using a lattice formulation.¹¹ The

¹¹The lattice size was $L = 16$, which roughly corresponds to $\Lambda = 8$ from the viewpoint of the number of degrees of freedom.

T	$\Lambda = 2$	$\Lambda = 3$	$\Lambda = 4$	$\Lambda = 5$	$\Lambda = 6$	$\Lambda = 7$	$\Lambda = 8$
1.0	3.489(33)	3.350(37)	3.217(41)	3.212(38)	3.172(35)	3.184(41)	3.138(53)
0.9	2.978(14)	2.810(18)	2.722(20)	2.659(33)	2.637(26)	2.651(43)	2.666(26)
0.8	2.498(13)	2.316(16)	2.222(16)	2.146(24)	2.114(24)	2.133(43)	2.132(25)
0.7	2.054(11)	1.868(15)	1.758(12)	1.689(24)	1.647(25)	1.627(27)	1.628(24)
0.6	1.675(11)	1.450(12)	1.342(17)	1.284(24)	1.208(23)	1.171(31)	1.209(21)
0.5	1.368(9)	1.128(12)	1.005(13)	0.948(22)	0.883(19)	0.857(27)	0.872(19)

Table 1: The results for the internal energy E/N^2 obtained with $N = 16$ at each T and Λ .

T	$\Lambda = \infty$, const. fit	$\Lambda = \infty$, linear fit
1.0	3.169(24)	3.091(82)
0.9	2.651(17)	2.680(86)
0.8	2.124(16)	2.104(75)
0.7	1.634(14)	1.565(123)
0.6	1.201(14)	1.203(110)
0.5	0.873(12)	0.832(98)

Table 2: The results for the internal energy E/N^2 in the continuum limit obtained by extrapolation to $\Lambda = \infty$ with the constant fit and the linear fit. The constant fit is performed using the data within $6 \leq \Lambda \leq 8$, whereas the linear fit is performed by fitting the data to $E/N^2 = a/\Lambda + b$ with the fitting range $4 \leq \Lambda \leq 8$ for $T = 1.0$, $5 \leq \Lambda \leq 8$ for $T = 0.9, 0.8$ and $6 \leq \Lambda \leq 8$ for $T = 0.7, 0.6, 0.5$.

values obtained from the same fit was $a = -0.90(26) \times 10$ and $p = 4.74(35)$. In ref. [18], a one-parameter fit with the power $p = 4.6$ fixed was also performed, and the coefficient was determined as $a = -5.58(1)$.

In order to clarify this discrepancy, we improve our previous analysis in ref. [18] by making extrapolations to $\Lambda = \infty$. In Fig. 1 (Left) we plot our results obtained for $N = 16$ against $1/\Lambda$. We tried both a linear extrapolation $E/N^2 = a + b/\Lambda$ and a constant fit. The values at each Λ and the values obtained by the extrapolations are given in Table 1 and 2, respectively. In Fig. 1 (Right), we plot the internal energy obtained by the extrapolations. The new results are consistent with the fit $E/N^2 = 7.41 T^{2.8} - 5.58 T^{4.6}$ obtained in ref. [18].

In Fig. 2 we plot the difference between the obtained internal energy and the leading prediction (2.13) from supergravity. The difference is normalized by the leading prediction as $y = (7.41 T^{2.8} - E/N^2)/7.41 T^{2.8}$ and it is plotted against $x = T^{1.8}$. The leading α' corrections correspond to a linear behavior towards the origin. Indeed we see a linear behavior for $T \leq 0.7$ consistent with the fit obtained in ref. [18]. On the other hand, the subleading terms are expected to show up as $y = a_1 x + a_2 x^{5/3} + a_3 x^2 + a_4 x^{7/3} + \dots$. The solid line and the dashed line are fits to $y = a_1 x + a_2 x^{5/3}$ using the data points within the range $0.5 \leq T \leq 0.7$ and $0.5 \leq T \leq 0.9$, respectively, obtained by the linear fit. In the latter case, the left-most data point obtained by the constant fit is slightly off the fitting

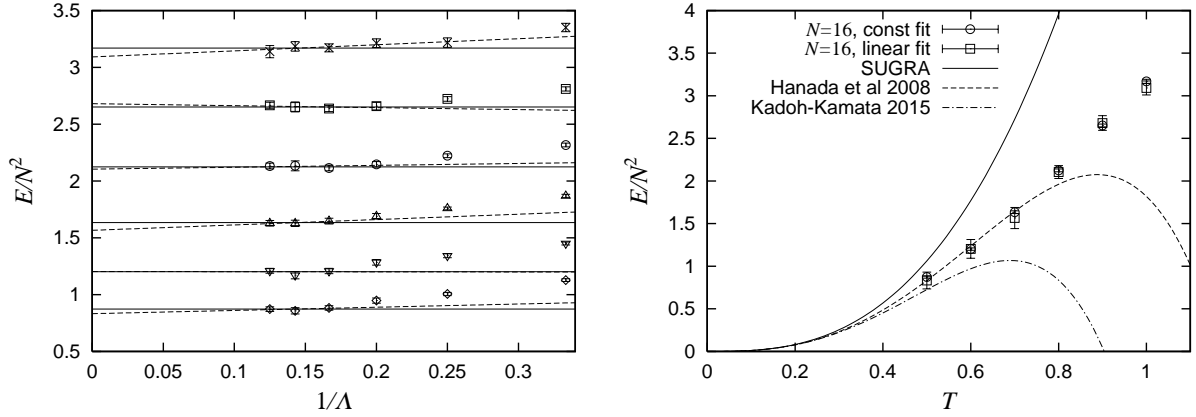


Figure 1: (Left) The internal energy E/N^2 for $N = 16$ is plotted against $1/\Lambda$ for $T = 0.5, 0.6, 0.7, 0.8, 0.9, 1.0$ from the bottom to the top. The solid and dashed lines represent fits to $E/N^2 = \text{const.}$ and $E/N^2 = a + b/\Lambda$, respectively. (Right) The internal energy obtained by extrapolation to $\Lambda = \infty$. The solid line represents the prediction of type IIA supergravity $E/N^2 = 7.41T^{2.8}$. The dashed line represents a fit $E/N^2 = 7.41T^{2.8} + aT^{4.6}$ with $a = -5.58(1)$ obtained in ref. [18]. The dash-dotted line represents a fit $E/N^2 = 7.41T^{2.8} + aT^p$ with $a = -0.90(26) \times 10$ and $p = 4.74(35)$ obtained in ref. [24].

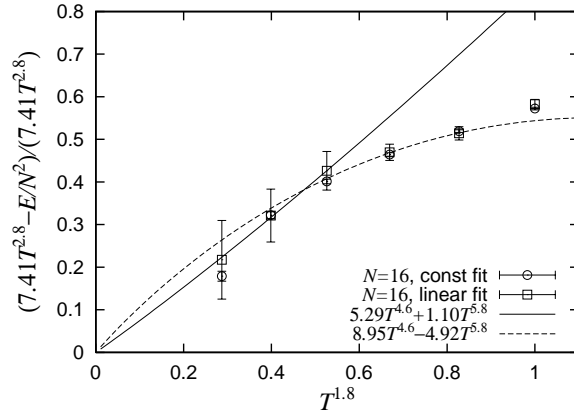


Figure 2: The quantity $y = (7.41T^{2.8} - E/N^2)/7.41T^{2.8}$ representing the deviation of the internal energy from the leading prediction from supergravity is plotted against $x = T^{1.8}$. The solid line and the dashed line represent fits to $y = a_1x + a_2x^{5/3}$ using the data within the range $0.5 \leq T \leq 0.7$ and $0.5 \leq T \leq 0.9$, respectively, obtained by the linear fit.

curve. However, this may be due to finite- N effects, which become more significant at lower temperature as is suggested from the $1/N$ expansion (2.20). In order to decide which fit is more appropriate, we clearly need more data at lower temperature with larger N .

4.2 Test including string loop corrections

In this section we test the gauge/gravity duality including string loop corrections. For that purpose, we need to study the D0-brane quantum mechanics at small N such as $N = 3, 4, 5$. As is mentioned at the end of section 3.2, the system has instability at small N associated with the flat directions in the action. In order to probe the instability, we define

$$R^2 \equiv \frac{1}{N\beta} \int_0^\beta dt \sum_{i=1}^9 \text{Tr}(X_i(t)^2) , \quad (4.1)$$

which represents the extent of the eigenvalue distribution of X_i 's. In Monte Carlo simulation, we prepare the initial configuration of $X_i(t)$ with small R^2 by giving each element a small Gaussian random number. At sufficiently low T , we observe that R^2 stabilizes as the simulation proceeds, and fluctuates around some value for a while and then starts to diverge. This behavior motivates us to consider the partition function (3.15), where R_{max}^2 is replaced by R^2 for simplicity.¹² What we do in practice is to add the potential term

$$V = \begin{cases} c |R^2 - R_{\text{cut}}^2| & \text{for } R^2 \geq R_{\text{cut}}^2 , \\ 0 & \text{for } R^2 < R_{\text{cut}}^2 , \end{cases} \quad (4.2)$$

to the action, where c and R_{cut}^2 are some parameters to be chosen appropriately.

Let us define the distribution of R^2 by

$$\rho(x) = \left\langle \delta(R^2 - x) \right\rangle , \quad (4.3)$$

where the expectation value is taken in the system with the potential (4.2). Figure 3 (Top-Left) shows the distribution $\rho(x)$ obtained from Monte Carlo simulation with $N = 4$, $T = 0.10$, $\Lambda = 10$, where we have set $c = 100$ and $R_{\text{cut}}^2 = 4.2$. There is a clear peak around $R^2 \sim 3.5$, which indicates the existence of the meta-stable bound states. The long tail at $R^2 \gtrsim 4$ represents the run-away behavior caused by the instability. In Fig. 3 (Top-Right) we plot the internal energy $E(x)/N^2$ obtained by averaging only over configurations with $R^2 < x$ for the same set of parameters. We see a clear plateau around $x \sim 4$, which confirms the argument given in section 3.2. Practically, we define the internal energy of the bound states by the local minimum of $E(x)/N^2$ in the plateau region.

The extent of the bound state can be identified as the lower end of the plateau region, which we denote as x_{min} . In practice, we obtain the value of x , at which $E(x)/N^2$ deviates from the local minimum by 5%, and similarly the value of x allowing 10% deviation. We use

¹²We consider that this does not make much difference because the fluctuation of $\sum_{i=1}^9 \text{Tr}(X_i(t)^2)$ as a function of t is typically small.

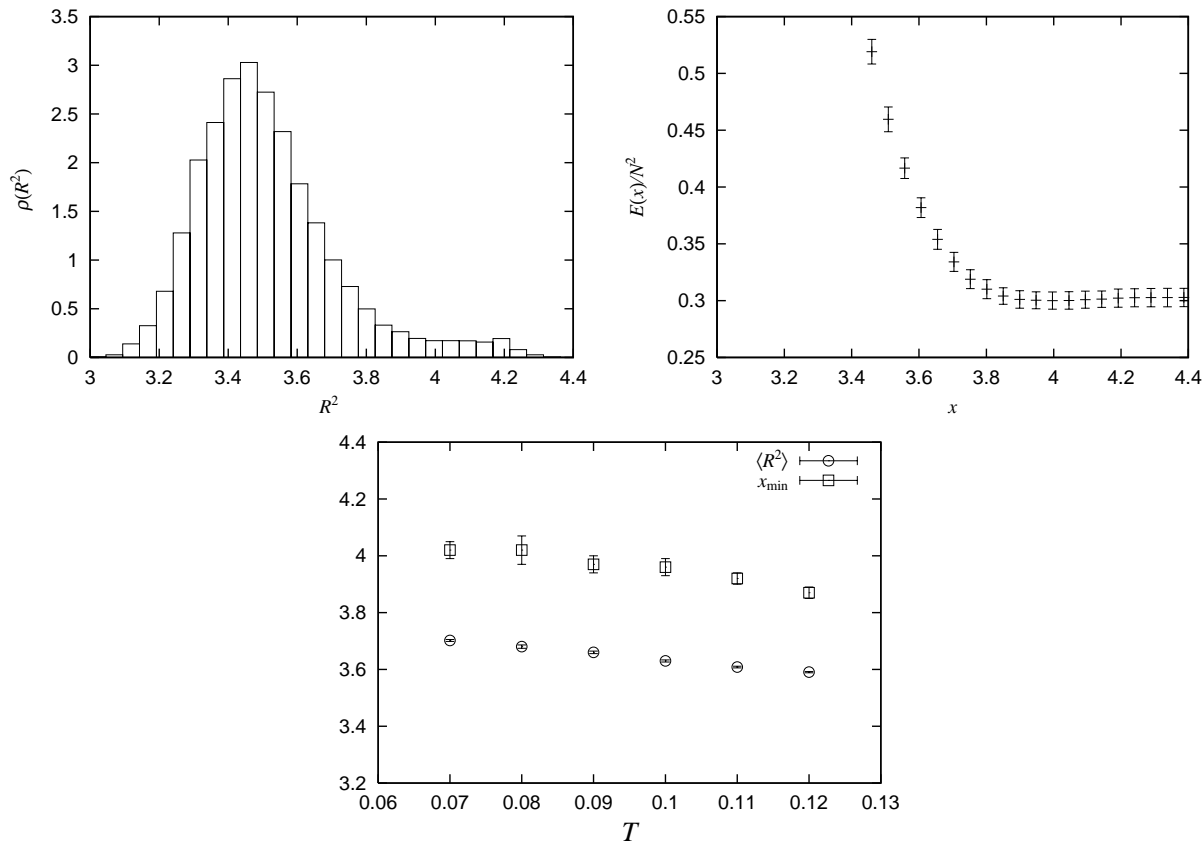


Figure 3: (Top-Left) The distribution of R^2 for $N = 4$, $T = 0.10$ and $\Lambda = 10$ using $c = 100$ and $R_{\text{cut}}^2 = 4.2$ in (4.2). (Top-Right) The function $E(x)/N^2$ for the same set of parameters. (Bottom) The extent of the bound states estimated by x_{\min} as described in the text is plotted as a function of T for $N = 4$ and $\Lambda = 16$. We also plot the expectation value $\langle R^2 \rangle$ obtained from configurations with $R^2 \leq x_{\min}$.

the average of the two values as an estimate of x_{\min} and the difference as an estimate of the ambiguity (“error”). In Fig. 3 (Bottom) we plot x_{\min} thus obtained as a function of T for $N = 4$ and $\Lambda = 16$ together with the expectation value $\langle R^2 \rangle$ obtained from configurations with $R^2 \leq x_{\min}$. We observe that both x_{\min} and $\langle R^2 \rangle$ increase as T is lowered. Note that the quantity $\langle R^2 \rangle$ at large N can be obtained without such a cutoff procedure, and it is a monotonically increasing function of T . (See Fig. 2 of ref. [35], for instance.)

Using the method explained above, we calculate the internal energy of the bound states for various N , T and Λ . We have studied $0.08 \leq T \leq 0.12$ for $N = 3$, $0.07 \leq T \leq 0.12$ for $N = 4$ and $0.08 \leq T \leq 0.11$ for $N = 5$. In Table 3, we present our results for the internal energy obtained at each N , T and Λ . We make an extrapolation to $\Lambda = \infty$ assuming that finite Λ corrections to the internal energy are given by $E = E_{\text{gauge}} + \text{const.}/\Lambda$, from which we extract the value E_{gauge} in the continuum limit. This extrapolation is performed using $8 \leq \Lambda \leq 16$ for $T \geq 0.10$ and $10 \leq \Lambda \leq 16$ for $T < 0.10$. Figure 4 (Left) shows the case

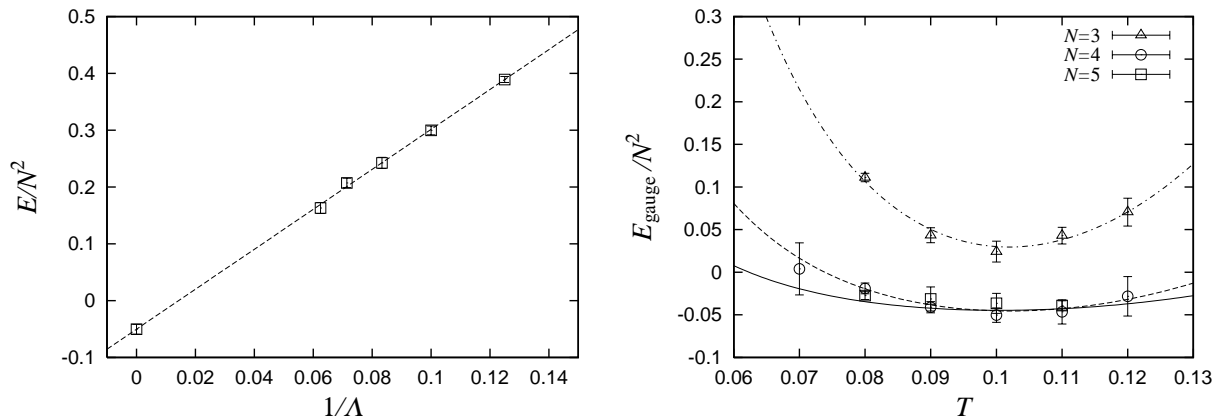


Figure 4: (Left) The internal energy of the bound states is plotted against $1/\Lambda$ for $N = 4$, $T = 0.10$. The straight line represents a fit to the behavior $E = E_{\text{gauge}} + \text{const.}/\Lambda$, and the value of E_{gauge} obtained by the fit is plotted at $\Lambda = \infty$. (Right) The internal energy E_{gauge}/N^2 obtained from our results by extrapolation to $\Lambda = \infty$ is plotted against T . The curves represent $E_{\text{gauge}}/N^2 = E_{\text{gravity}}/N^2 + (cT^{-2.6} + \tilde{c}T^p)/N^4$, where the parameters c , \tilde{c} and p are obtained by fits as described at the end of section 4.2. The solid, dashed and dash-dotted lines correspond to $N = 5$, 4 and 3, respectively.

of $N = 4$, $T = 0.10$. In Fig. 4 (Right), we plot our results for E_{gauge}/N^2 obtained in the continuum limit by extrapolation to $\Lambda = \infty$. (The explicit values are given in the right most column of Table 3.) The curves in this plot are explained at the end of this section.

Let us compare our results with the prediction from the gravity side. Since the α' corrections are negligible in the temperature regime investigated here, we can compare our results with (2.19), which we denote as E_{gravity}/N^2 in what follows. Let us also expand the internal energy of the bound states obtained on the gauge theory side as

$$\frac{E_{\text{gauge}}}{N^2} = c_0(T) + \frac{c_1(T)}{N^2} + \frac{c_2(T)}{N^4} + \dots \quad (4.4)$$

If the gauge/gravity duality holds, the first and the second terms above should coincide with those in (2.19), namely, $c_0(T) = 7.41 T^{14/5}$ and $c_1(T) = -5.77 T^{2/5}$. In other words, the difference of the two quantities E_{gauge} and E_{gravity} should behave as

$$\frac{1}{N^2}(E_{\text{gauge}} - E_{\text{gravity}}) = \frac{c_2(T)}{N^4} + O\left(\frac{1}{N^6}\right). \quad (4.5)$$

In Fig. 5 (Left), we plot $(E_{\text{gauge}} - E_{\text{gravity}})/N^2$ against $1/N^4$, which can be nicely fitted by a straight line passing through the origin. We also observe a similar behavior for other values of T . Thus, we confirm the behavior (4.5), which implies that the gauge/gravity duality holds including the leading quantum gravity correction. In Fig. 5 (Right), we plot E_{gauge}/N^2 against $1/N^2$, which can be fitted nicely by $E_{\text{gauge}}/N^2 = 7.41 T^{2.8} - 5.76 T^{0.4}/N^2 + \text{const.}/N^4$ as expected from the gauge/gravity duality. On the other hand, we also find that the

N	T	$\Lambda = 8$	$\Lambda = 10$	$\Lambda = 12$	$\Lambda = 14$	$\Lambda = 16$	$\Lambda = \infty$
5	0.11	0.353(9)	0.273(13)	0.225(17)	0.181(19)	0.160(29)	-0.039(6)
5	0.10	0.375(8)	0.290(15)	0.228(15)	0.200(16)	0.178(20)	-0.037(11)
5	0.09	0.397(6)	0.323(8)	0.269(10)	0.218(10)	0.193(13)	-0.031(14)
5	0.08	0.417(6)	0.349(6)	0.287(11)	0.242(18)	0.205(24)	-0.027(5)
4	0.12	0.366(6)	0.297(7)	0.242(11)	0.213(11)	0.153(10)	-0.028(23)
4	0.11	0.374(7)	0.279(8)	0.227(10)	0.199(10)	0.165(12)	-0.047(14)
4	0.10	0.389(5)	0.300(8)	0.242(10)	0.207(8)	0.163(10)	-0.050(8)
4	0.09	0.405(4)	0.332(5)	0.267(7)	0.224(9)	0.195(12)	-0.041(7)
4	0.08	0.422(4)	0.365(5)	0.298(7)	0.254(9)	0.223(11)	-0.019(6)
4	0.07	0.442(3)	0.375(4)	0.329(4)	0.289(5)	0.245(6)	0.004(30)
3	0.12	0.407(6)	0.327(8)	0.295(9)	0.264(13)	0.243(14)	0.071(16)
3	0.11	0.397(6)	0.332(8)	0.284(8)	0.238(11)	0.220(10)	0.043(10)
3	0.10	0.396(4)	0.323(7)	0.280(7)	0.242(10)	0.201(8)	0.024(12)
3	0.09	0.411(5)	0.344(5)	0.293(8)	0.257(6)	0.240(17)	0.049(8)
3	0.08	0.426(4)	0.355(9)	0.313(7)	0.288(15)	0.263(14)	0.111(5)

Table 3: The results for the internal energy at each N , T and Λ . In the right most column, we also present the results in the continuum limit obtained by extrapolation to $\Lambda = \infty$.

$O(1/N^4)$ term is actually comparable to the $O(1/N^2)$ term. This is related to the fact that the coefficient of the $1/N^4$ term grows at low T as we see below.

As an alternative analysis, we fit our results for each T with

$$E_{\text{gauge}}/N^2 = 7.41T^{2.8} + c_1/N^2 + c_2/N^4, \quad (4.6)$$

where c_1 and c_2 are fitting parameters. In Fig. 6, we plot the values of c_1 obtained by the two-parameter fit as a function of T , which agree well with the behavior $c_1 = -5.76T^{0.4}$ expected from the gravity side.

Let us also discuss the T dependence of c_2 . In Fig. 6 (Right) we plot the value of c_2 obtained by fitting our data to (4.6) with $c_1 = -5.76T^{0.4}$ fixed. From the prediction from the gravity side (2.18), we find that $c_2 = cT^{-2.6} + \dots$, where the leading behavior is determined by the $(m, n) = (5, 2)$ term in (2.18). We can actually fit our results to $c_2 = cT^{-2.6} + \tilde{c}T^p$ with $c = 0.032(2)$, $\tilde{c} = 0.51(64) \times 10^5$ and $p = 3.7(6)$, where the second term $\tilde{c}T^p$ is meant to represent all the subleading terms phenomenologically.¹³ Therefore we consider that the T dependence of c_2 is also consistent with the prediction from the gravity side. The curves in Fig. 4 (Right) represent $E_{\text{gauge}}/N^2 = E_{\text{gravity}}/N^2 + (cT^{-2.6} + \tilde{c}T^p)/N^4$ with c , \tilde{c} and p obtained above.

¹³The value for \tilde{c} obtained by the fit looks huge, but it is actually compensated by the high power of T within the temperature region investigated here.

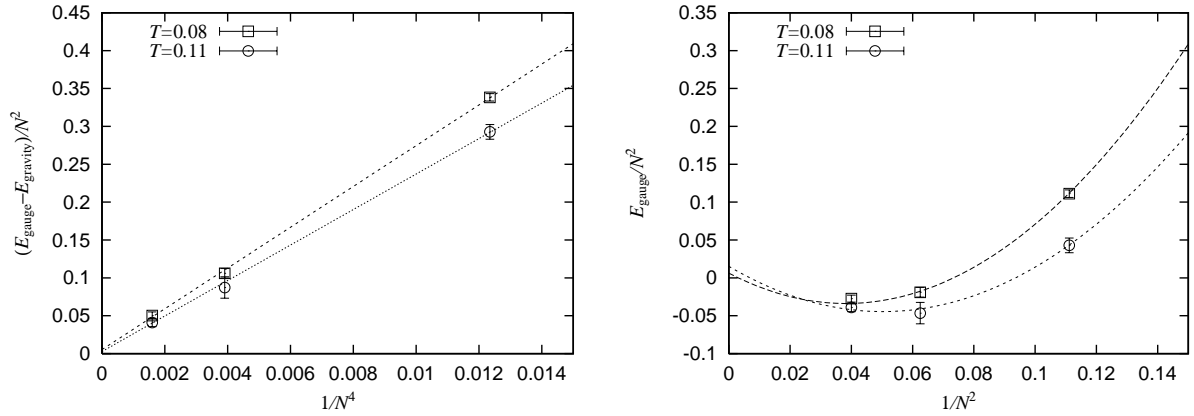


Figure 5: (Left) The difference $(E_{\text{gauge}} - E_{\text{gravity}})/N^2$ between the internal energy obtained by the gauge theory and that predicted from the gravity side is plotted against $1/N^4$, where the straight lines represent fits to a linear behavior. (Right) The internal energy E_{gauge}/N^2 obtained by the gauge theory is plotted against $1/N^2$. The dashed lines represent fits to the behavior $E_{\text{gauge}}/N^2 = 7.41 T^{2.8} - 5.76 T^{0.4}/N^2 + \text{const.}/N^4$, which is expected from the gravity side.

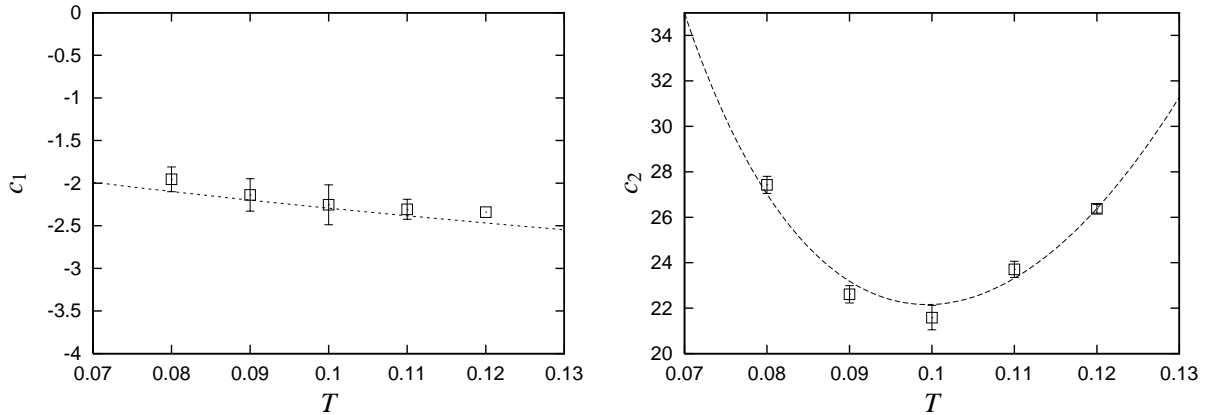


Figure 6: (Left) The parameter c_1 obtained by fitting our results to $E_{\text{gauge}}/N^2 = 7.41T^{2.8} + c_1/N^2 + c_2/N^4$ is plotted against T . The dashed line represents the behavior $f(T) = -5.76 T^{0.4}$ expected from the gravity side. The data point for $T = 0.12$ does not have an error bar since we have only two data points ($N = 3$ and $N = 4$) for the two-parameter fit. (Right) The parameter c_2 obtained by fitting our results to $E_{\text{gauge}}/N^2 = 7.41T^{2.8} - 5.76 T^{0.4}/N^2 + c_2/N^4$ is plotted against T . The dashed line represents a fit to the behavior $c_2 = cT^{-2.6} + \tilde{c}T^p$ with $c = 0.032(2)$, $\tilde{c} = 0.51(64) \times 10^5$ and $p = 3.7(6)$,

5 Summary and discussions

In this paper we have performed numerical tests of the gauge/gravity duality conjecture including the α' and string loop corrections by using N D0-branes at finite temperature. On the gravity side, these are described by the black 0-brane geometry. The leading part is obtained by the supergravity solution, and the α' and string loop corrections can be taken into account perturbatively, which leads to the internal energy of the black 0-brane given by eq. (2.20). On the gauge theory side, the D0-branes are described by the matrix quantum mechanics, which has been studied by Monte Carlo simulation.

In the large- N limit, the string loop corrections can be neglected on the gravity side and the internal energy is given by eq. (2.16). We have improved our previous analysis in ref. [18] by performing extrapolations to the continuum limit. While our new results are still consistent with the fit obtained previously, we have also suggested an alternative fit obtained by taking into account the higher order α' corrections. More calculations at low temperature with larger N are required for a definite conclusion to be reached.

We have also provided a test of the gauge/gravity duality including string loop corrections. In order to see the string loop corrections, we need to study the D0-brane system with small N such as $N = 3, 4, 5$. This is difficult because of the instability associated with the flat directions of the potential. At low temperature, however, we observe from Monte Carlo simulations that the bound states of D0-branes become meta-stable. We investigate the thermodynamics of these meta-stable bound states by introducing a cutoff on the extent of the D0-branes. Indeed we find that the internal energy becomes independent of the cutoff within a finite region. From this behavior, we were able to obtain the internal energy of the meta-stable bound states as a function of the temperature, which turns out to be consistent with the result (2.19) obtained recently on the gravity side including the leading string loop corrections. To our knowledge, this is the first dynamical evidence that suggests that the gauge/gravity duality holds at finite N . (See ref. [41] for studies on kinematical aspects of the duality including $1/N$ corrections.)

A particularly interesting future direction would be to investigate the D0-brane system at even lower temperature with larger N . On the gravity side, it is expected that the black 0-brane geometry becomes unstable, and undergoes a transition to a black hole moving along the eleventh direction [8] due to the Gregory-Laflamme instability [42]. This corresponds to a Schwarzschild black hole in eleven dimensions, where the Hawking radiation becomes a non-negligible effect unlike the case investigated in this paper. The transition temperature has been obtained as $T_c = 0.574N^{-5/9} + 0.707N^{-11/9} + \dots$ including the leading quantum correction [43]. If one can see this transition in the dual gauge theory, one should also be able to investigate the conjecture that the same matrix quantum mechanics actually describes M theory nonperturbatively [3].

Acknowledgements

The authors would like to thank Sinya Aoki, Sean Hartnoll, Issaku Kanamori, Hikaru Kawai, Erich Poppitz, Andreas Schäfer, Stephen Shenker, Leonard Susskind, Masaki Tezuka, Akiko Ueda and Mithat Ünsal for valuable discussions and comments. M. H. is supported by the Hakubi Center for Advanced Research, Kyoto University and by the National Science Foundation under Grant No. PHYS-1066293. M. H. and Y. H. are partially supported by the Ministry of Education, Science, Sports and Culture, Grant-in-Aid for Young Scientists (B), 25800163, 2013 (M. H.) and 24740140, 2012 (Y. H.). The work of G. I. is supported in part by Program to Disseminate Tenure Tracking System, MEXT, Japan. The work of J. N. is supported in part by Grant-in-Aid for Scientific Research (No. 20540286, 23244057) from Japan Society for the Promotion of Science. Computations were carried out on PC cluster systems in KEK and Osaka University Cybermedia Center (the latter being provided by the HPCI System Research Project, project ID:hp120162).

A Hawking radiation in type IIA supergravity

The internal energy of the black 0-brane is affected by the Hawking radiation. In order to estimate the strength of this effect, we consider the Stefan-Boltzmann law in 10-dimensional spacetime

$$\frac{d\tilde{E}}{dt} = \sigma A_H \tilde{T}^{10} = \sigma A_H \lambda^{\frac{10}{3}} T^{10}, \quad (\text{A.1})$$

where σ is some constant and A_H is the area of the event horizon evaluated in the Einstein frame as

$$A_H = e^{-2\phi} V_{S^8} (\ell_s H^{\frac{1}{2}} U)^8 \Big|_{\tilde{v}_0} = \frac{2(2\pi)^6 \sqrt{\pi}}{7\sqrt{15}} \ell_s^{14} \lambda^2 U_0^{\frac{9}{2}} = \frac{2(2\pi)^6 \sqrt{\pi}}{7\sqrt{15}} a_1^{-\frac{9}{5}} \ell_s^{14} \lambda^2 T^{\frac{9}{5}} \quad (\text{A.2})$$

using the constant a_1 given in (2.12). In terms of dimensionless quantities (2.14), the energy loss per unit time is expressed as

$$\frac{dE}{d(\lambda^{1/3}t)} = \sigma' (\ell_s \lambda^{\frac{1}{3}})^{14} T^{\frac{59}{5}}, \quad \sigma' = \frac{2(2\pi)^6 \sqrt{\pi}}{7\sqrt{15}} a_1^{-\frac{9}{5}} \sigma. \quad (\text{A.3})$$

Since the coefficient vanishes in the $\ell_s \rightarrow 0$ limit, the energy loss through the Hawking radiation can be neglected in the present calculation. This conclusion is understandable since the near horizon limit corresponds to a particular case of the near extremal limit as we mentioned below eq. (2.10).

B Leading higher derivative corrections at one loop

In this appendix, we briefly review the derivation [10] of the internal energy (2.19) including the leading higher derivative correction at the one-loop level, which corresponds to the $(m, n) = (3, 1)$ term in the effective action (2.1).

Including the correction, the 0-brane solution is modified and given with an asymptotically flat metric as

$$\begin{aligned}
ds^2 &= -H_1^{-1}H_2^{\frac{1}{2}}F_1dt^2 + H_2^{\frac{1}{2}}F_1^{-1}dr^2 + H_2^{\frac{1}{2}}r^2d\Omega_8^2, \quad e^\phi = H_2^{\frac{3}{4}}, \quad C = \sqrt{1+\alpha^7}(H_2H_3)^{-\frac{1}{2}}dt, \\
H_i &= 1 + \frac{r_-^7}{r^7} + \frac{\gamma}{r_-^6\alpha^{13}} \left\{ h_i\left(\frac{r}{r_-}\right) + \alpha^7 \hat{h}_i\left(\frac{r}{r_-}\right) \right\}, \quad F_1 = 1 - \frac{r_-^7\alpha^7}{r^7} + \frac{\gamma}{r_-^6\alpha^6} f_1\left(\frac{r}{r_-}\right),
\end{aligned} \tag{B.1}$$

where $\gamma = \frac{\pi^2}{2^{11}3^2}\ell_s^6 g_s^2$. The four functions $h_i(x)$ and $f_1(x)$ are uniquely determined as¹⁴

$$\begin{aligned}
h_1(x) &= \frac{1302501760}{9x^{34}} - \frac{57462496}{x^{27}} + \frac{12051648}{13x^{20}} - \frac{4782400}{13x^{13}} \\
&\quad - \frac{3747840}{x^7} + \frac{4099200}{x^6} - \frac{1639680(x-1)}{(x^7-1)} + 117120\left(18 - \frac{23}{x^7}\right)I(x), \\
h_2(x) &= \frac{19160960}{x^{34}} - \frac{58528288}{x^{27}} + \frac{2213568}{13x^{20}} - \frac{1229760}{13x^{13}} \\
&\quad - \frac{2108160}{x^7} + \frac{2459520}{x^6} + 1054080\left(2 - \frac{1}{x^7}\right)I(x), \\
h_3(x) &= \frac{361110400}{9x^{34}} - \frac{59840032}{x^{27}} - \frac{24021312}{13x^{20}} - \frac{58072000}{13x^{13}} \\
&\quad - \frac{2108160}{x^7} + \frac{2459520}{x^6} + 117120\left(18 - \frac{41}{x^7}\right)I(x), \\
f_1(x) &= -\frac{1208170880}{9x^{34}} + \frac{161405664}{x^{27}} + \frac{5738880}{13x^{20}} + \frac{956480}{x^{13}} + \frac{3747840}{x^7} + \frac{819840}{x^7}I(x),
\end{aligned} \tag{B.2}$$

and the three functions $\hat{h}_i(x)$ are expressed as

$$\begin{aligned}
\hat{h}_1(x) &= \frac{1035722240}{9x^{27}} + \frac{1721664}{x^{20}} + \frac{22955520}{13x^{13}} + \frac{1912960}{x^6} - 1639680\frac{x-1}{x^7-1} + 234240I(x), \\
\hat{h}_2(x) &= -\hat{h}_3(x) = \frac{94330880}{9x^{27}} + \frac{655872}{x^{20}} + \frac{13117440}{13x^{13}} + \frac{2186240}{x^6} + 1873920I(x),
\end{aligned} \tag{B.3}$$

where

$$\begin{aligned}
I(x) &= \log \frac{x^7(x-1)}{x^7-1} - \sum_{n=1,3,5} \cos \frac{n\pi}{7} \log \left(x^2 + 2x \cos \frac{n\pi}{7} + 1 \right) \\
&\quad - 2 \sum_{n=1,3,5} \sin \frac{n\pi}{7} \left\{ \tan^{-1} \left(\frac{x + \cos \frac{n\pi}{7}}{\sin \frac{n\pi}{7}} \right) - \frac{\pi}{2} \right\}.
\end{aligned} \tag{B.4}$$

¹⁴In fact, the term $\frac{3747840}{x^7}$ in the function $f_1(x)$ was dropped in ref. [9] by imposing a stronger boundary condition, although we actually need it to satisfy the asymptotic flatness of the solution. This does not affect the final results for physical quantities such as entropy since they depend on $f_1(x)$ only through the combination $7f_1(1) + f_1'(1)$.

Using the black 0-brane solution including the leading quantum correction (B.1), we can obtain various quantities associated with the solution. The Hawking temperature is given by

$$\tilde{T} = \frac{7\alpha^{\frac{5}{2}}}{4\pi r_- \sqrt{1+\alpha^7}} \left[1 + \frac{\gamma}{r_-^6 \alpha^6} \left\{ \left(\frac{8}{7} - \frac{1}{2(1+\alpha^7)} \right) f_1(\alpha) + \frac{1}{7} f_1'(1) - \frac{1}{2(1+\alpha^7)} h_1(1) \right\} \right] \quad (\text{B.5})$$

up to the linear order in γ , while the mass and the charge are evaluated, respectively, as

$$\tilde{M} = \frac{V_{S^8}}{2\kappa_{10}^2} \{ r_-^7 (7 + 8\alpha^7) - 16865280\gamma r_- \alpha \}, \quad \tilde{Q} = \frac{V_{S^8}}{2\kappa_{10}^2} 7r_-^7 \sqrt{1+\alpha^7}, \quad (\text{B.6})$$

which shows that the charge is not affected by quantum corrections.

After taking the near horizon limit, the dimensionless temperature becomes

$$T = a_1 U_0^{\frac{5}{2}} (1 + \epsilon a_2 U_0^{-6}), \quad a_2 = \frac{9}{14} f_1(1) + \frac{1}{7} f_1'(1) - \frac{1}{2} h_1(1), \quad \epsilon = \frac{\pi^6}{2^7 3^2 N^2}, \quad (\text{B.7})$$

and the dimensionless internal energy becomes

$$\begin{aligned} \frac{E}{N^2} &= \frac{V_{S^8}}{2\kappa_{10}^2 N^2 \lambda^{\frac{1}{3}}} \left\{ \frac{1 + 8\sqrt{1+\alpha^7}}{1 + \sqrt{1+\alpha^7}} r_-^7 \alpha^7 - 16865280\gamma r_- \alpha \right\} \\ &= \frac{18}{7^3} a_1^2 (U_0^7 - 3747840 \epsilon U_0) \\ &= \frac{18}{7^3} a_1^2 \left\{ a_1^{-\frac{14}{5}} T^{\frac{14}{5}} - \epsilon \left(\frac{14}{5} a_2 + 3747840 \right) a_1^{-\frac{2}{5}} T^{\frac{2}{5}} \right\} \\ &= 7.41 T^{\frac{14}{5}} - \frac{5.77}{N^2} T^{\frac{2}{5}}. \end{aligned} \quad (\text{B.8})$$

This is consistent with the result derived in ref. [9] using the first law of the black hole thermodynamics.

C Derivation of the formula for the internal energy

In this appendix we derive the formula (3.14), which is used to calculate the internal energy by Monte Carlo simulation. Let us first rewrite the internal energy $E = -\frac{\partial}{\partial \beta} \ln Z$ as

$$E = -\frac{1}{Z(\beta)} \lim_{\Delta\beta \rightarrow 0} \frac{Z(\beta') - Z(\beta)}{\Delta\beta}, \quad (\text{C.1})$$

where $\beta' = \beta + \Delta\beta$, and represent $Z(\beta')$ for later convenience as

$$Z(\beta') = \int [\mathcal{D}A']_{\beta'} [\mathcal{D}X']_{\beta'} [\mathcal{D}\psi']_{\beta'} e^{-S'}, \quad (\text{C.2})$$

where S' is obtained from S given in (3.1) by replacing $\beta, t, A(t), X_i(t), \psi_\alpha(t)$ with $\beta', t', A'(t'), X'_i(t'), \psi'_\alpha(t')$. In order to relate $Z(\beta')$ to $Z(\beta)$, we consider the transformation

$$t' = \frac{\beta'}{\beta} t, \quad A'(t') = \frac{\beta}{\beta'} A(t), \quad X'_i(t') = \sqrt{\frac{\beta'}{\beta}} X_i(t), \quad \psi'(t') = \psi(t), \quad (\text{C.3})$$

where the constant factors are motivated on dimensional grounds. As for the path integral measure, we impose $[\mathcal{D}X']_{\beta'} = [\mathcal{D}X]_\beta$, $[\mathcal{D}\psi']_{\beta'} = [\mathcal{D}\psi]_\beta$ and $[\mathcal{D}A']_{\beta'} = [\mathcal{D}A]_\beta$, which corresponds to subtracting the internal energy for the free theory in the definition (C.1). Under this transformation, the kinetic term in S' reduces to that in S , but the interaction term transforms non-trivially as

$$\int_0^{\beta'} dt' \text{Tr} \left([X'_i(t'), X'_j(t')] \right)^2 = \left(\frac{\beta'}{\beta} \right)^3 \int_0^\beta dt \text{Tr} \left([X_i(t), X_j(t)] \right)^2, \quad (\text{C.4})$$

$$\int_0^{\beta'} dt \text{Tr} \left(\psi_\alpha(t') [X'_i(t'), \psi'_\beta(t')] \right) = \left(\frac{\beta'}{\beta} \right)^{3/2} \int_0^\beta dt \text{Tr} \left(\psi_\alpha [X_i(t), \psi_\beta(t)] \right). \quad (\text{C.5})$$

This gives us the relation

$$Z(\beta') = Z(\beta) \left\{ 1 - \frac{\Delta\beta}{\beta} \left(3\langle S_{\text{b,int}} \rangle + \frac{3}{2}\langle S_{\text{f,int}} \rangle \right) + \mathcal{O}((\Delta\beta)^2) \right\}, \quad (\text{C.6})$$

where $S_{\text{b,int}}$ and $S_{\text{f,int}}$ represent the bosonic and fermionic part of the interaction terms, respectively. Plugging these into (C.1), we get

$$E = \frac{3}{\beta} \left(\langle S_{\text{b,int}} \rangle + \frac{1}{2}\langle S_{\text{f,int}} \rangle \right). \quad (\text{C.7})$$

Thus we are able to express the internal energy E in terms of the expectation values, which can be calculated by Monte Carlo simulation. However, the second term $\langle S_{\text{f,int}} \rangle$ is computationally demanding since it involves fermionic matrices. This motivates us to rewrite it in terms of quantities involving bosonic matrices only.

For that purpose, we consider a change of variables $X_i(t) \mapsto e^\epsilon X_i(t)$ in the partition function. The kinetic term $S_{\text{b,kin}}$ for the bosonic matrices $X_i(t)$ in (3.1) transforms as $S_{\text{b,kin}} \mapsto e^{2\epsilon} S_{\text{b,kin}}$, whereas the interaction terms transform as $S_{\text{b,int}} \mapsto e^{4\epsilon} S_{\text{b,int}}$ and $S_{\text{f,int}} \mapsto e^\epsilon S_{\text{f,int}}$. The path integral measure for the bosonic matrices $X_i(t)$ transforms as $dX \mapsto e^{9\epsilon\{N^2(2\Lambda+1)-1\}} dX$, where the “ -1 ” is due to the fact that the trace part in the constant mode of $X_i(t)$ does not appear in the action and hence should be omitted. Since the partition function should be invariant under the change of variables, we obtain the identity

$$9\{N^2(2\Lambda+1)-1\} = 2\langle S_{\text{b,kin}} \rangle + 4\langle S_{\text{b,int}} \rangle + \langle S_{\text{f,int}} \rangle. \quad (\text{C.8})$$

Solving this equation for $\langle S_{\text{f,int}} \rangle$, and plugging it into (C.7), we obtain the formula (3.14).

When we add the potential (4.2) to the action, the formula (3.14) is modified by an extra term coming from the potential. However, in the parameter region investigated in

this work, the extra term turns out to be negligible as we briefly discuss below. For this reason, we use the formula (3.14) with or without the potential (4.2).

For simplicity, we consider introducing the constraint $R^2 \leq R_{\text{cut}}^2$, which corresponds to inserting an extra factor $\theta(R_{\text{cut}}^2 - R^2)$ in the integrand of the path integral (3.10). Under the transformation (C.3), R^2 defined in (4.1) transforms as

$$\frac{1}{\beta'} \int_0^{\beta'} dt' \text{Tr} X'_i(t')^2 = \left(\frac{\beta'}{\beta}\right) \frac{1}{\beta} \int_0^{\beta} dt \text{Tr} X_i(t)^2 . \quad (\text{C.9})$$

Therefore, the extra factor transforms as

$$\begin{aligned} & \theta\left(R_{\text{cut}}^2 - \frac{1}{N\beta'} \int_0^{\beta'} dt' \text{Tr} X'_i(t')^2\right) \\ &= \theta\left(R_{\text{cut}}^2 - \frac{1}{N\beta} \int_0^{\beta} dt \text{Tr} X_i(t)^2\right) - \frac{\Delta\beta}{\beta} R_{\text{cut}}^2 \delta\left(R_{\text{cut}}^2 - \frac{1}{N\beta} \int_0^{\beta} dt \text{Tr} X_i(t)^2\right) , \end{aligned} \quad (\text{C.10})$$

omitting the higher order terms in $\Delta\beta$. Therefore, the relation (C.6) is modified as

$$Z(\beta') = Z(\beta) \left\{ 1 - \frac{\Delta\beta}{\beta} \left(3\langle S_{\text{b,int}} \rangle + \frac{3}{2}\langle S_{\text{f,int}} \rangle + R_{\text{cut}}^2 \rho(R_{\text{cut}}^2) \right) + \mathcal{O}((\Delta\beta)^2) \right\} , \quad (\text{C.11})$$

where $\rho(x)$ is defined by (4.3) in the system with the constraint $R^2 \leq R_{\text{cut}}^2$. Thus, (C.7) is modified as

$$E = \frac{3}{\beta} \left(\langle S_{\text{b,int}} \rangle + \frac{1}{2}\langle S_{\text{f,int}} \rangle \right) + \frac{1}{\beta} R_{\text{cut}}^2 \rho(R_{\text{cut}}^2) . \quad (\text{C.12})$$

Let us evaluate the extra term in the case shown in Fig. 3 (Top-Left). Here we have $N = 4$, $\beta = 1/T = 10$, $R_{\text{cut}}^2 = 4.2$ and $\rho(R_{\text{cut}}^2) \sim 0.2$, and hence the quantity E/N^2 receives a contribution from the extra term of the order of $\frac{4.2 \times 0.2}{10 \times 4^2} \sim 0.005$, which may be neglected in the scale of Fig. 4 (Left). In general, the extra term is suppressed by the factor $\rho(R_{\text{cut}}^2)$, which is small if the system is stable enough.

References

- [1] J. Polchinski, “Dirichlet branes and Ramond-Ramond charges”, Phys. Rev. Lett. **75**, 4724 (1995), [hep-th/9510017].
- [2] A. Strominger, C. Vafa, “Microscopic origin of the Bekenstein-Hawking entropy”, Phys. Lett. B **379**, 99 (1996), [hep-th/9601029].
- [3] T. Banks, W. Fischler, S. H. Shenker and L. Susskind, “M theory as a matrix model: a conjecture”, Phys. Rev. D **55**, 5112 (1997), [hep-th/9610043].
- [4] N. Ishibashi, H. Kawai, Y. Kitazawa and A. Tsuchiya, “A large N reduced model as superstring”, Nucl. Phys. B **498**, 467 (1997), [hep-th/9612115].

- [5] R. Dijkgraaf, E. P. Verlinde and H. L. Verlinde, “Matrix string theory,” Nucl. Phys. B **500**, 43 (1997), [hep-th/9703030].
- [6] H. Itoyama and A. Tokura, “USp(2k) matrix model: Nonperturbative approach to orientifolds,” Phys. Rev. D **58**, 026002 (1998), [hep-th/9801084].
- [7] J. M. Maldacena, “The large N limit of superconformal field theories and supergravity,” Adv. Theor. Math. Phys. **2**, 231 (1998), [Int. J. Theor. Phys. **38**, 1113 (1999)], [hep-th/9711200].
- [8] N. Izhaki, J. M. Maldacena, J. Sonnenschein and S. Yankielowicz, “Supergravity and the large N limit of theories with sixteen supercharges”, Phys. Rev. D **58**, 046004 (1998), [hep-th/9802042].
- [9] Y. Hyakutake, “Quantum near-horizon geometry of a black 0-brane”, PTEP **3** (2014), 033B04, [arXiv:1311.7526[hep-th]].
- [10] Y. Hyakutake, “Quantum M-wave and black 0-brane”, JHEP **1409**, (2014) 075, [arXiv:1407.6023[hep-th]].
- [11] B. de Wit, J. Hoppe and H. Nicolai, “On the Quantum Mechanics of Supermembranes”, Nucl. Phys. B **305**, 545 (1988).
- [12] D. N. Kabat and G. Lifschytz, “Approximations for strongly coupled supersymmetric quantum mechanics”, Nucl. Phys. B **571**, 419 (2000), [hep-th/9910001].
- [13] D. N. Kabat, G. Lifschytz and D. A. Lowe, “Black hole thermodynamics from calculations in strongly coupled gauge theory”, Int. J. Mod. Phys. A **16**, 856 (2001), [Phys. Rev. Lett. **86**, 1426 (2001)], [hep-th/0007051].
- [14] D. N. Kabat, G. Lifschytz and D. A. Lowe, “Black hole entropy from nonperturbative gauge theory”, Phys. Rev. D **64**, 124015 (2001), [hep-th/0105171].
- [15] N. Iizuka, D. N. Kabat, G. Lifschytz and D. A. Lowe, “Probing black holes in nonperturbative gauge theory”, Phys. Rev. D **65**, 024012 (2002), [hep-th/0108006].
- [16] K. N. Anagnostopoulos, M. Hanada, J. Nishimura and S. Takeuchi, “Monte Carlo studies of supersymmetric matrix quantum mechanics with sixteen supercharges at finite temperature”, Phys. Rev. Lett. **100**, 021601 (2008), [arXiv:0707.4454 [hep-th]].
- [17] M. Hanada, A. Miwa, J. Nishimura and S. Takeuchi, “Schwarzschild radius from Monte Carlo calculation of the Wilson loop in supersymmetric matrix quantum mechanics”, Phys. Rev. Lett. **102**, 181602 (2009), [arXiv:0811.2081 [hep-th]].
- [18] M. Hanada, Y. Hyakutake, J. Nishimura and S. Takeuchi, “Higher derivative corrections to black hole thermodynamics from supersymmetric matrix quantum mechanics”, Phys. Rev. Lett. **102**, 191602 (2009), [arXiv:0811.3102 [hep-th]].

- [19] M. Hanada, J. Nishimura, Y. Sekino and T. Yoneya, “Direct test of the gauge-gravity correspondence for Matrix theory correlation functions”, JHEP **1112**, 020 (2011), [arXiv:1108.5153 [hep-th]].
- [20] M. Hanada, J. Nishimura, Y. Sekino and T. Yoneya, “Monte Carlo studies of Matrix theory correlation functions”, Phys. Rev. Lett. **104**, 151601 (2010), [arXiv:0911.1623 [hep-th]].
- [21] M. Hanada, Y. Hyakutake, G. Ishiki and J. Nishimura, “Holographic description of a quantum black hole on a computer”, Science **344**, 882 (2014), [arXiv:1311.5607 [hep-th]].
- [22] S. Catterall and T. Wiseman, “Black hole thermodynamics from simulations of lattice Yang-Mills theory”, Phys. Rev. D **78**, 041502 (2008), [arXiv:0803.4273 [hep-th]].
- [23] S. Catterall and T. Wiseman, “Extracting black hole physics from the lattice”, JHEP **1004**, 077 (2010), [arXiv:0909.4947 [hep-th]].
- [24] D. Kadoh and S. Kamata, “Gauge/gravity duality and lattice simulations of one dimensional SYM with sixteen supercharges,” arXiv:1503.08499 [hep-lat].
- [25] V. G. Filev and D. O’Connor, “The BFSS model on the lattice,” arXiv:1506.01366 [hep-th].
- [26] D. J. Gross and E. Witten, “Superstring modifications of Einstein’s equations,” Nucl. Phys. B **277**, 1 (1986) .
- [27] D. J. Gross and J. H. Sloan, “The quartic effective action for the heterotic string,” Nucl. Phys. B **291**, 41 (1987).
- [28] M. B. Green, J. G. Russo and P. Vanhove, “Non-renormalisation conditions in type II string theory and maximal supergravity”, JHEP **0702** (2007) 099, [hep-th/0610299].
- [29] A. A. Tseytlin, “ R^4 -terms in 11-dimensions and Conformal anomaly of (2,0) theory”, Nucl. Phys. **B584**, 233 (2000), [hep-th/0005072].
- [30] K. Becker and M. Becker, “Supersymmetry breaking, M theory and fluxes”, JHEP **0107**, 038 (2001), [hep-th/0107044].
- [31] K. Peeters, P. Vanhove and A. Westerberg, “Supersymmetric higher-derivative actions in ten and eleven dimensions, the associated superalgebras and their formulation in superspace”, Class. Quant. Grav. **18**, 843 (2001), [hep-th/0010167].
- [32] Y. Hyakutake and S. Ogushi, “Higher derivative corrections to eleven dimensional supergravity via local supersymmetry”, JHEP **0602**, 068 (2006), [hep-th/0601092].

- [33] Y. Hyakutake, “Toward the Determination of $R^3 F^2$ Terms in M-theory”, *Prog. Theor. Phys.* **118**, 109 (2007), [hep-th/0703154].
- [34] M. Hanada, J. Nishimura and S. Takeuchi, “Non-lattice simulation for supersymmetric gauge theories in one dimension”, *Phys. Rev. Lett.* **99**, 161602 (2007), [arXiv:0706.1647 [hep-lat]].
- [35] N. Kawahara, J. Nishimura and S. Takeuchi, “High temperature expansion in supersymmetric matrix quantum mechanics,” *JHEP* **0712**, 103 (2007), [arXiv:0710.2188 [hep-th]].
- [36] S. Catterall and T. Wiseman, “Towards lattice simulation of the gauge theory duals to black holes and hot strings,” *JHEP* **0712**, 104 (2007) [arXiv:0706.3518 [hep-lat]].
- [37] N. Kawahara, J. Nishimura and S. Takeuchi, “Phase structure of matrix quantum mechanics at finite temperature,” *JHEP* **0710**, 097 (2007) [arXiv:0706.3517 [hep-th]].
- [38] A. V. Smilga, “Comments on thermodynamics of supersymmetric matrix models”, *Nucl. Phys. B* **818**, 101 (2009), [arXiv:0812.4753].
- [39] M. Hanada, S. Matsuura, J. Nishimura and D. Robles-Llana, “Nonperturbative studies of supersymmetric matrix quantum mechanics with 4 and 8 supercharges at finite temperature,” *JHEP* **1102**, 060 (2011) [arXiv:1012.2913 [hep-th]].
- [40] E. Brezin, C. Itzykson, G. Parisi and J. B. Zuber, *Commun. Math. Phys.* **59**, 35 (1978).
- [41] A. Arabi Ardehali, J. T. Liu, P. Szepietowski, “The spectrum of IIB supergravity on $AdS_5 \times S^5/Z_3$ and a $1/N^2$ test of AdS/CFT,” *JHEP* **1306**, 024 (2013), [arXiv:1304.1540 [hep-th]].
- [42] R. Gregory and R. Laflamme, “Black strings and p-branes are unstable,” *Phys. Rev. Lett.* **70**, 2837 (1993), [hep-th/9301052].
- [43] Y. Hyakutake, “Boosted quantum black hole and black string in M-theory, and quantum correction to Gregory-Laflamme instability,” *JHEP* **1509**, 067 (2015), [arXiv:1503.05083 [gr-qc]].